https://doi.org/10.5194/esd-2021-65
Preprint. Discussion started: 30 July 2021

Earth System Dynamics
Discussions

The Mediterranean climate change hotspot in the CMIP5 and CMIP6 projections

Josep Cos[1], Francisco Doblas-Reyes[1,2], Martin Jury[1], Raül Marcos[1], Pierre-Antoine Bretonnière[1], and Margarida Samsó[1]

[1]Earth Sciences Department, Barcelona Supercomputing Center (BSC), Barcelona, Spain.
[2]Institució Catalana de Recerca i Estudis Avançats (ICREA), Barcelona, Spain

Correspondence: Josep Cos (josep.cos@bsc.es)

Abstract. The increased warming trend and precipitation decline in the Mediterranean region makes it a climate change hotspot. We compare projections of multiple CMIP5 and CMIP6 historical and scenario simulations to quantify the impacts of the already changing climate in the region. In particular, we investigate changes in temperature and precipitation during the 21st century following scenarios RCP2.6, SSP1-2.6, RCP4.5, SSP2-4.5, RCP8.5 and SSP5-8.5, as well as the HighResMIP high resolution experiments. A model weighting scheme is applied to obtain constrained estimates of projected changes, which accounts for historical model performance and inter-independence of the multi-model ensembles, using an observational ensemble as reference. Results indicate a robust and significant warming over the Mediterranean region along the 21st century over all seasons, ensembles and experiments. The Mediterranean amplified warming with respect to the global mean is mainly found during summer. The temperature changes vary between CMIPs, being CMIP6 the ensemble that projects a stronger warming. Contrarily to temperature projections, precipitation changes show greater uncertainties and spatial heterogeneity. However, a robust and significant precipitation decline is projected over large parts of the region during summer for the high emission scenario. While there is less disagreement in projected precipitation between CMIP5 and CMIP6, the latter shows larger precipitation declines in some regions. Results obtained from the model weighting scheme indicate increases in CMIP5 and reductions in CMIP6 warming trends, thereby reducing the distance between both multi-model ensembles.

1 Introduction

The Mediterranean region (10º W, 40º E, 30º N, 45º N) (Iturbide et al., 2020) is located between the arid and warm North-African climate and the humid and mild European continental climate (Cramer et al., 2018). The influence of the surrounding oceans, their interaction with the land surface and the general atmospheric circulation characteristics in mid-latitudes partly explain the contrast between these climates (Boé and Terray, 2014).

Global warming is not homogeneous, and Lionello and Scarascia (2018) suggest that the Mediterranean region is a climate change hotspot. Consequently, adaptation to the changing climate threats is paramount to the countries located around the Mediterranean Sea (Gleick, 2014; Cramer et al., 2018), which live in a complex and diverse socioeconomic situation and have severe vulnerabilities to climate change and variability (Barros et al., 2014). The observed warming in the Mediterranean region

https://doi.org/10.5194/esd-2021-65
Preprint. Discussion started: 30 July 2021

during the last decades is expected to continue and grow larger than the global warming mean (Lionello and Scarascia, 2018). Additionally, total precipitation declines have been observed during the late 20th century (Longobardi and Villani, 2010), and projected by different multi-model ensembles for the 21st century (Paeth et al., 2017; Zittis et al., 2019). Nevertheless, longer periods are required to robustly assess historic precipitation trends to account for interdecadal and interannual variability influences (Peña-Angulo et al., 2020). Characteristics of the projected Mediterranean climate change have been linked to thermodynamic sources such as land-ocean warming contrast and lapse rate change in summer (Brogli et al., 2019), or to dynamical processes such as the changes in upper-tropospheric large-scale flow in winter (Tuel and Eltahir, 2020).

Numerical models are used to estimate future climate change. Accounting for the physical processes and interactions in each climate subsystem (atmosphere, biosphere, cryosphere, hydrosphere and land-surface), global climate models (GCMs) aim to project the state of the future climate system. Model runs over long historical or future periods are driven by natural forcings (i.e. solar irradiance and volcanic aerosols) and anthropogenic emissions that alter the greenhouse gas (GHG) concentrations, leading to changes in the radiative forcing. (Hawkins and Sutton, 2011). GCMs are developed by a number of institutions who always apply the same physical principles but might use slightly different assumptions. This opens the door to performing the same experiments with multiple tools leading to more robust estimates. Modelling uncertainty can be sampled by ensembling various models (Tebaldi and Knutti, 2007), while running the same model multiple times under the same experiment samples internal variability (Hawkins and Sutton, 2011). To make the results comparable, intercomparison projects where several models perform standardized experiments have been organised by the international community. (Meinshausen et al., 2011; Riahi et al., 2016). The main community effort is the Coupled Model Intercomparison Project (CMIP). In this study we consider the latest two CMIP phases, CMIP5 and CMIP6 (Taylor et al., 2012; Eyring et al., 2016), and explore their similarities and differences over the Mediterranean region. The almost ten years between CMIP5 and CMIP6 allowed for improvements in the modelling of certain earth system processes such as cloud feedbacks, aerosol forcings or aerosol-cloud interactions (Voosen, 2019; Wang et al., 2021).

CMIP experiments were performed with a large set of models and therefore show many differences in projected changes due to internal variability and the diverse model designs used by the modelling teams. By weighting single model runs according to their performance in simulating the observed past allows constraining the climate modelling uncertainty and obtaining a potentially more accurate estimate of regional climate change signals. Various studies have used different subsetting/weighting approaches such as emergent constraints (Cox et al., 2018; Hall et al., 2019; Tokarska et al., 2020), performance-based model subsets (McSweeney et al., 2015; Langenbrunner and Neelin, 2017; Herger et al., 2019) or model weighting accounting for performance and independence (Knutti et al., 2017; Lorenz et al., 2018; Brunner et al., 2019). The latter approach has been used in this study as it additionally considers the interdependencies existing between the models.

This study evaluates and quantifies the Mediterranean climate change hotspot for each season over the 21st century by looking into surface air temperature and precipitation changes and how they relate to global-mean and large-scale changes. We consider three different emission scenarios to assess the impact of anthropogenic emission uncertainties over the Mediterranean climate. The CMIP5 and CMIP6 multi-model ensembles are used to estimate the climate change signal, its uncertainty and

https://doi.org/10.5194/esd-2021-65
Preprint. Discussion started: 30 July 2021

Earth System Dynamics
Discussions

to illustrate the differences between the two experiments in the region. Finally, a weighting method is applied to each CMIP ensemble based on the assumption of model performance and independence to obtain more robust projections.

Section 2 describes the climate models and observational data used, and explains the methods to quantify climate change and weight the projection members. The climate change hotspot in the Mediterranean and the weighted and unweighted projected changes are presented in 3, while these results are discussed in section 4. Section 5 concludes and raises questions for further investigation.

2 Data & Methods

2.1 Model data

This study is based on the CMIP5 and CMIP6 historical and future climate projections experiments. The historical CMIP5 experiments span from 1850 to 2005 (Taylor et al., 2012) and from 1850 to 2014 in CMIP6 (Eyring et al., 2016). The future projections are a continuation of the historical simulations, and we have used runs spanning until year 2100. The variables are monthly mean near-surface air temperature (TAS), precipitation rate (PR) and sea-level pressure (PSL). The latter is used to weight the ensemble members (see section 2.3).

The increasing computational power over time has allowed for increased model resolution and complexity, which leads to the expectation that models have improved from CMIP5 to CMIP6. Addtionally, we have used the High Resolution Model Intercomparison Project (HighResMIP), a CMIP6 endorsed MIP (Haarsma et al., 2016), aiming to compare lower and higher resolution versions of the same global models. The historical and future HighResMIP periods span from 1950 to 2014 and 2015 to 2050, respectively. Though only a subset of the CMIP6 models contributed to HighResMIP, this smaller ensemble has been also considered in this study to assess the impact of increasing model resolution on the Mediterranean climate.

Three radiative forcing scenarios are used to account for uncertainty in future emissions: the CMIP5 Representative Concentration Pathways (RCPs; (van Vuuren et al., 2011)) 2.6, 4.5 and 8.5 and the CMIP6 Shared Socioeconomic Pathways (SSPs; (Riahi et al., 2016)) 1-2.6, 2-4.5 and 5-8.5. The mangnitudes 2.6, 4.5 and 8.5 (in Wm^{-2}) represent the 2100 global radiative forcing in comparison to the pre-industrial era. However, even if the radiative forcing at the end of the century is the same in both RCPs and SSPs, the path to reach it can differ substantially, leading to differences in the projected climate (Wyser et al., 2020). One of the main differences between the SSPs and RCPs is that the former has a compatible socioeconomic scenario associated to each forcing scenario, SSP1 being based on sustainability, inclusive development and inequality reduction, SSP2 representing a middle of the road scenario, where slow progress is made in achieving sustainable development goals and with a mild decline in resource and energy use, and SSP5 based on a fossil-fueled development, rapid technological progress and economic growth (Riahi et al., 2016; O'Neill et al., 2016). The results from CMIP5 and CMIP6 sharing the same 2100 radiative forcing will be displayed together for simplicity, but the reader should always bear in mind that the evolution of GHG concentrations differs between them. HighResMIP is only available for the scenario SSP5-8.5 for future projections.

Many of the models have more than one member, meaning that the model runs have been started with different initial-conditions leading to diverging climate trajectories. The aim of having multiple members is to sample the uncertainty that

https://doi.org/10.5194/esd-2021-65
Preprint. Discussion started: 30 July 2021

Earth System Dynamics Discussions

arises from internal variability (Lehner et al., 2020; Deser et al., 2020). Having multi-member models means that the multi-model ensembles are super-ensembles. A summary of the simulations performed by each model used and for every scenario can be found in Appendix A.

2.2 Observational data

We use observational references to compare the model experiments to the observed past and to derive performance weights of ensemble members. Multiple observational products are used containing both reanalysis (ERA5 and JRA55) and gridded observations (GPCC, CRU, BerkeleyEarth and HadSLP2) to account for observational uncertainty. A summary of the observational datasets used is found in Table 1. JRA55 will not be displayed in the time series plots as it overestimates the precipitation over the Mediterranean during the period 1958-1978 (Tsujino et al., 2018).

Table 1. Observational references summary.

Name	Type	Institute	Variables	Reference
JRA55	Reanalysis	Japan Meteorological Agency (JMA)	TAS, PR, PSL	(Kobayashi et al., 2015)
ERA5	Reanalysis	European Centre for Medium-Range Weather Forecasts (ECMWF)	TAS, PSL	(Hersbach et al., 2020)
CRU (v4.04)	Gridded observations	University of East Anglia (UEA)	TAS, PR	(Harris et al., 2020)
GPCC (v2018)	Gridded observations	Deutscher Wetterdienst (DWD)	PR	(Schamm et al., 2014)
BerkeleyEarth	Gridded observations	Berkeley Earth	TAS	(Rohde et al., 2013)
HadSLP2	Gridded observations	Met Office (UKMO)	PSL	(Allan and Ansell, 2006)

2.3 Methods

All calculations have been performed using the Earth System Model Evaluation Tool (ESMValTool). ESMValTool is a community framework that facilitates the processing of generic climate datasets, allowing for reproducibility of results (Righi et al., 2020).

TAS and PR are only assessed over land to highlight the impact of climate change over populated regions. This avoids values over sea influencing results over land when the regridding is performed, i.e. TAS behaves differently over land than over sea due to differences in the thermodynamic properties of the surfaces, while PR over sea should not have an impact on freshwater resources over land.

The baseline periods 1986-2005 and 1980-2014 are the reference to assess the models performance against observations. The shorter 1986-2005 period (from Collins et al. (2013)) serves as a baseline for the calculation of climate change signals. The longer reference period (35 years) is used to compute historical trends, as 20-year trends are considered to be too heavily influenced by internal variability (Merrifield et al., 2020; Peña-Angulo et al., 2020). The reason for using the older 1986-2005 20-year period instead of the more recent 1995-2014 (Brunner et al., 2020) is to avoid CMIP5's historical period ending in 2005 to overlap with the corresponding scenario projection runs that start in 2006. Three future periods are considered to assess projected changes: near-term (2021-2040), mid-term (2041-2060) and long-term (2081-2100). Only the near-term period is available for HighResMIP as the future experiment ends in 2050.

https://doi.org/10.5194/esd-2021-65
Preprint. Discussion started: 30 July 2021

Earth System Dynamics
Discussions

All datasets are regridded to a $1^o \times 1^o$ grid using a conservative interpolation method to allow the comparison between different models and observational references. The height differences between the model orography and the evaluation grid implies that TAS must be corrected (by means of the 6.49 K/km standard lapse rate) whenever absolute climatologies are used (Weedon et al., 2011; Dennis, 2014).

To assess the seasonal dependence of climate change over the Mediterranean region, results are computed for December-January-February (DJF), March-April-May (MAM), June-July-August (JJA) and September-October-November (SON).

Differences and trends along the time coordinate are the main computations performed on models and observations in this study. Differences are computed subtracting the 20-year climatology reference period from the target period, which we refer to as changes from the baseline period. As GCMs are known to have biases, using differences allows for a more easily interpretable comparison of the responses among models and between models and observations (Garfinkel et al., 2020). Trends are defined by the linear ordinary least square regression fit with time as independent variable.

The statistical significance of TAS and PR mean changes and the degree of agreement between models are used to assess the uncertainty and robustness of the multi-model ensemble results. A climate change signal is considered robust when at least 80 % of the models agree on the sign of change (Collins et al., 2013). A change in the multi-model mean is considered significant when it is beyond the threshold of a two-tailed t-Student test at the 95% confidence level. The historical and future ensemble mean change and their inter-model standard deviations are used to compute the t-statistic.

It has been argued that more robust projections could be obtained by giving more weight to members with good performance (Knutti et al., 2017). Therefore, historical simulations are compared against the observational ensemble mean and more weight is given to those members that better reproduce the observed climate i.e. weighting them by performance. Another aspect that can be taken into account when weighting a multi-model ensemble is the independence between members. Giving equal weight to all members (one model one vote) is not a fair approach as some share model formulations (either because their runs belong to the same model or because their models share similarities), and would be over-represented in the ensemble. An independence weighting method is applied to correct this issue.

Using the approach developed in Lorenz et al. (2018), Brunner et al. (2020) and Merrifield et al. (2020), we use equation (1) to give a weight w_i to each member i in the projections ensemble. The distances (measured with the root mean squared error, RMSE) D_i between member i and the observational reference inform the performance weight, and the distance S_{ij} between member i and every other member j from the multi-model ensemble informs the independence weight. σ_s and σ_d are the independence and performance shape parameters, respectively. The mean of the observational ensemble is used as the observational reference.

$$w_i = \frac{e^{-\left(\frac{D_i}{\sigma_d}\right)^2}}{1 + \sum_{j \neq i}^{M} e^{-(\frac{S_{ij}}{\sigma_s})^2}} \quad (1)$$

The weighting method accounts for different performance and independence diagnostics (trends, differences, variabilities and climatologies) to avoid weighting members that could match the performance and independence criteria of a single diagnostic just by chance. The diagnostics used to evaluate the distances D_i and S_{ij} are different, as Merrifield et al. (2020)

https://doi.org/10.5194/esd-2021-65
Preprint. Discussion started: 30 July 2021

suggests. The aim when evaluating performance is to give weight to members that resemble the observed past in a more faithful way. Differently, the aim of weighting for independence is to clearly identify members that behave in a similar way. The variables used to compute the diagnostics are TAS and PSL (Merrifield et al., 2020). The performance diagnostics are the surface temperature difference with respect to the reference period (TAS-DIFF), the surface temperature interannual standard deviation (TAS-STD); the surface temperature linear trend (TAS-TREND), the sea-level pressure difference with respect to the reference period (PSL-DIFF), and the sea-level pressure interannual standard deviation (PSL-STD). The independence diagnostics are the 20-year PSL and TAS climatologies (PSL-CLIM and TAS-CLIM). The diagnostics are computed over the period 1980-2014 (Brunner et al., 2020).

The shape parameters are constant values that inform if the distance, obtained from comparing two diagnostics, is enough to downweight a member (σ_d) or if it is close enough to determine the dependency between members (σ_s). Each multi-model ensemble, season and scenario has its own shape parameters associated. Appendix B explains in further detail the meaning of the shape parameters, the methods used to compute them and the diagnostics to determine performance and independence.

3 Results

Apart from the figures displayed in this section and the supplementary material, additional ones generated during the study can be found in a shiny app in the following link https://earth.bsc.es/shiny/medprojections-shiny_app/.

3.1 The Mediterranean as a climate change hotspot

Figure 1 compares warming differences of the high radiative forcing scenarios of CMIP5 and CMIP6 over the Mediterranean with respect to the 1986-2005 global mean for winter, summer and the annual means. For precipitation, Mediterranean change is compared to the 30º N-45º N latitudinal belt mean. The Mediterranean region shows a higher annual temperature increase than the global mean. When accounting for seasonal differences, the highest amplifications are visible for summer over the Iberian Peninsula and the Balkans. CMIP5 and CMIP6 agree on the regions showing the highest amplified warming, but CMIP6 projects larger amplification magnitudes. There is agreement between both CMIPs in the distribution and magnitude of the winter warming amplification, which is small and even negative in the northwest part of the domain. While projections agree on a precipitation increase in the 30º N-45º N latitudinal belt for the long-term period (Lionello and Scarascia, 2018), the Mediterranean region shows precipitation decreases. The largest amplified drying shifts latitudinally from the south of the Mediterranean region in winter to the north in summer. The most affected region in summer is projected to be the southwest of the Iberian Peninsula. Both CMIPs agree on the patterns of change, but CMIP6 dries more and faster in the amplified drying regions, and projects larger precipitation increases in regions where the hotspot has a negative sign such as the southeast of the domain.

The TAS and PR differences increase in magnitude from the mid to the long-term, while the spatial pattern remains the same, indicating that the climate in the Mediterranean changes faster than the larger scale means when forced by the 8.5 Wm^{-2} scenarios. The low emission scenario instead shows a hotspot weakening from the mid to the long-term as the warming

https://doi.org/10.5194/esd-2021-65
Preprint. Discussion started: 30 July 2021

Earth System Dynamics
Discussions

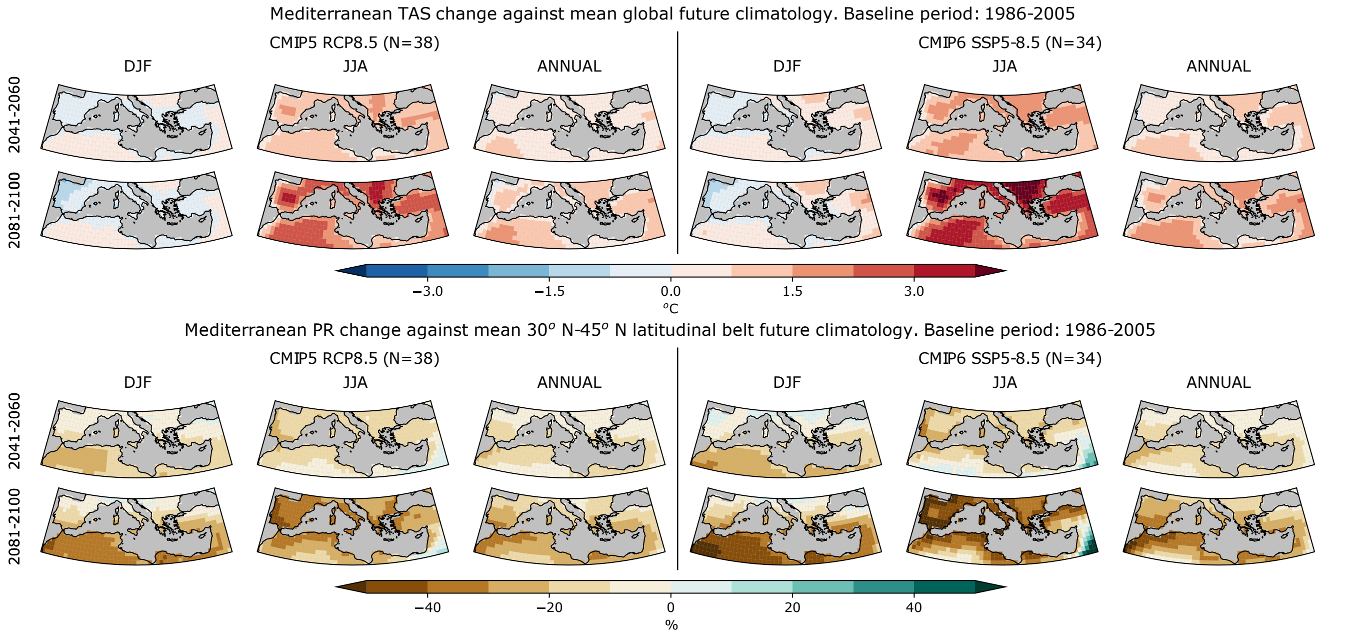

Figure 1. Mediterranean region TAS (upper rows) and PR (lower rows) change differences with respect to the mean global temperature change and the mean 30° N-45° N latitudinal belt precipitation change. The changes are evaluated against the 1986-2005 mean for the 2041-2060 (1st and 3rd row) and 2081-2100 periods (2nd and 4th row). The differences are shown for the CMIP5 (left) and CMIP6 (right) winter, summer and annual mean projections (columns) under the high emission scenario RCP8.5 and SSP5-8.5, respectively. N indicates the number of models included in the ensemble mean.

amplification is reduced and the precipitation differences are maintained (see Fig. S1). The weakening of the hotspot under the low emission scenario will be further explored below.

Even though CMIP6 is projecting a larger warming and drying amplification than CMIP5, Fig. 2 shows agreement between CMIP5 and CMIP6 in the relation of global and local warming. This indicates that CMIP6 is not enhancing the hotspot with respect to CMIP5, but rather the higher amplified warming in the Mediterranean is the result of a globally warmer multi-model ensemble. For DJF, additional warming over the Mediteranean is almost zero with respect to the global mean. Contrastingly for JJA, additional warming over the Mediteranean is about 1.6 $\times$ higher than the global mean warming. This relationship appears to be linearly maintained for higher global warming levels, i.e. with time and GHG-concentrations. CMIP6 shows a slightly larger slope for the rest of seasons (not shown).

In spite of this strong agreement in additional local warming, CMIP5 and CMIP6 show some differences in projected precipitation over the Mediterranean in comparison to the 30° N-45° N latitudinal belt precipitation changes (see Fig. S2). The aggregated difference between the precipitation increase in the latitudinal belt and the precipitation decline in the Mediterranean is larger for CMIP6 which suggests that CMIP6 projects a more extreme hotspot than CMIP5 regarding precipitation. Conclusions must be drawn carefully, as Fig. S3 shows how the precipitation along the belt is not homogeneous, which could

https://doi.org/10.5194/esd-2021-65
Preprint. Discussion started: 30 July 2021

Earth System Dynamics
Open Access
Discussions

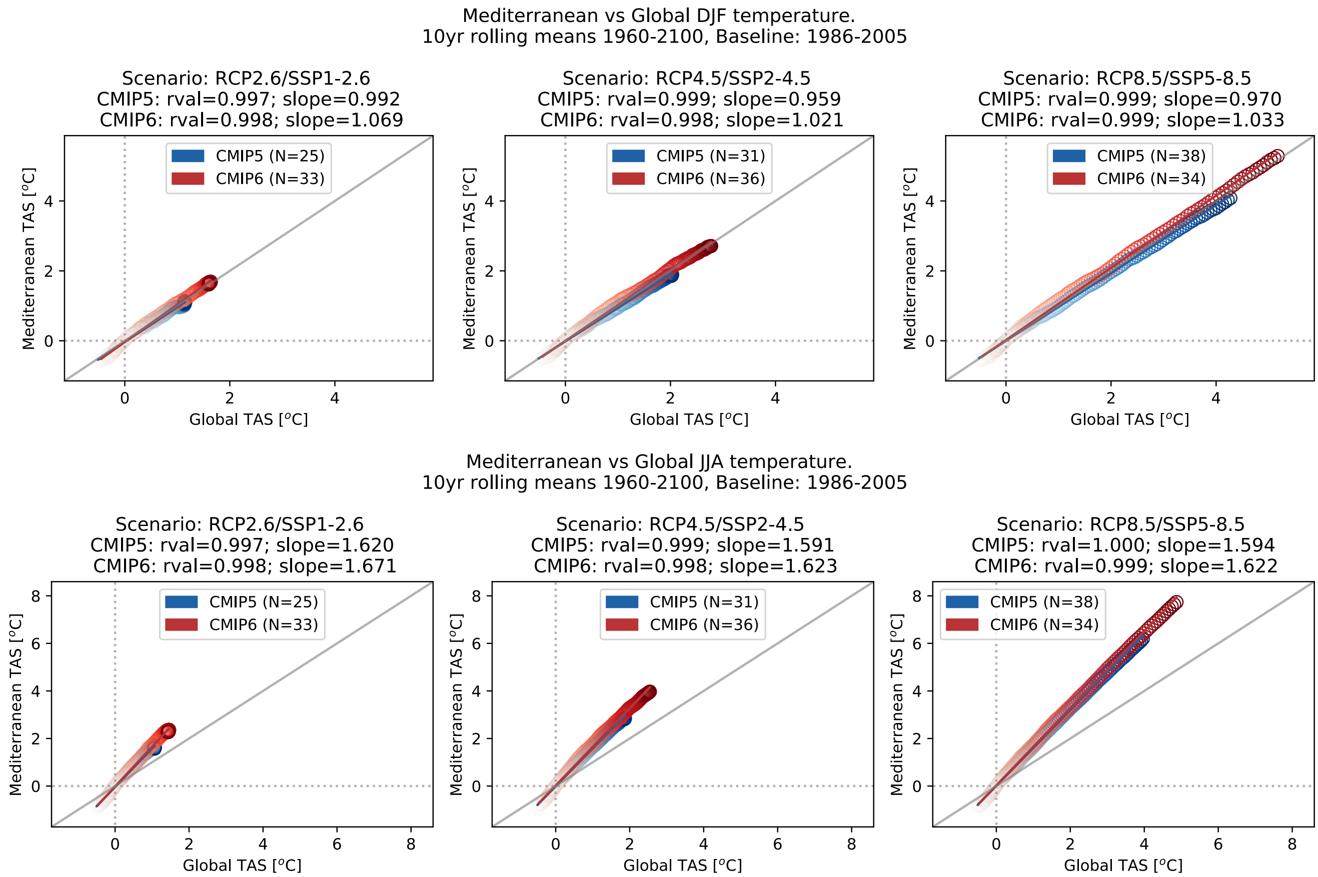

Figure 2. Mediterranean region warming against global warming for the three scenarios (columns) shown in winter (top row) and summer (bottom row) for the CMIP5 and CMIP6 ensemble means. Each dot represents a 10 year mean change beginning from 1960-1969 (light coloring) until 2091-2100 (opaque coloring). The changes are computed with 1986-2005 as baseline. An ordinary least squares linear regression is computed and the slope and r values are shown. N indicates the number of models included in the ensemble mean.

lead to negative and positive precipitation changes canceling out. The figure highlights more extreme CMIP6 precipitation changes in the latitudinal band and increases of over 30 % in Asia and over the Pacific as opposed to CMIP5. Nevertheless, there is agreement between both ensembles on the spatial distribution of PR changes.

Following a second approach to assess the precipitation hotspot, Fig. S4 shows changes in precipitation for the Mediterranean region against the global mean warming, the ensemble that dries faster for the same magnitude of global warming is CMIP5. Coming back to the hotspot weakening, the low emission scenario panels show more clearly how a recovery of the precipitation decline is projected following mitigation. For the rest of the scenarios, the projected amplified warming, combined with an anomalous precipitation decline, makes the Mediterranean a climate change hotspot (Lionello and Scarascia, 2018).

https://doi.org/10.5194/esd-2021-65
Preprint. Discussion started: 30 July 2021

Earth System Dynamics
Discussions

3.2 Unweighted future projections

We compare CMIP and HighResMIP ensemble TAS and PR trends to the observational ensemble trends between 1980 and 2014 as an indication of model performance over the Mediterranean. The spread of the multi-model ensemble trends contain the observational ensemble trends (see Fig. S5). Mostly, for the remaining seasons, the observations fall inside the 90 % spread of the multi-model ensemble historical runs (not shown). The historical multi-model ensemble spread of temperature trends is notably larger than that of the observational ensemble. CMIP6 past warming trends are generally larger than CMIP5. The inter-model spread for the precipitation projections is large for all ensembles and usually has both negative and positive trends (e.g DJF CMIP5 precipitation trend range from -0.092 to 0.097 $mm\,day^{-1}\,decade^{-1}$ for the 5th and 95th percentiles, respectively). HighResMIP TAS trends are contained within the CMIP6 ensemble, but the PR high-resolution (HR) models trends display outliers in summer (Fig. S5.d). The agreement between the different observational products in past warming trends is shown in Fig. S7 (columns 1 and 5). While the general warming patterns are similar there are some notable differences over the Balkans and Western Asia. The figure also highlights the need of considering multiple observational sources, as historical trends differ both in magnitudes and spatial patterns.

Figure 3(a,c) shows projected multi-model ensemble summer and winter TAS and PR changes under three scenarios and three time horizons over the Mediterranean. The CMIP6 ensemble always shows larger temperature increases than CMIP5. Inter-model spread for the end of the century is larger for CMIP6 than CMIP5. CMIP6 projects summer temperatures to increase by over 7.4 ºC (90 % within 5.6 ºC to 9.1 ºC) until the end of the century under the high emission scenario and 2.3 ºC (90 % within 1.2 ºC to 3.3 ºC) under for the low emission scenario (Fig. 3). CMIP5 shows a mean summer warming of 5.9 ºC by the end of the century (90 % within 4.1 ºC to 7.7 ºC) under RCP8.5 and 1.6 ºC (90 % within 0.3 ºC to 2.5 ºC) under RCP2.6. Also for the remaining seasons, CMIP6 shows a larger warming and larger intermodel spread than CMIP5 (not shown). As expected, the projection spread broadens with time as models diverge. Summer remains the season with the largest temperature increase. For winter and the high emission scenario, 90 % of CMIP6 models project a temperature change between 3.3 and 6.8 ºC (CMIP5: 2.7 ºC to 5.0 ºC). HighResMIP HR and low-resolution (LR) projections are contained within the CMIP5 and CMIP6 distributions (only near-term, see Fig. S5.c). Due to the small size of the HighResMIP ensemble further conclusions can't be withdrawn.

In contrast to temperature, CMIP5 and CMIP6 show the same mean summer precipitation declines of -33 % by the end of the century under the high emission scenario, respectively (Fig. 3.c). CMIP6 has a wider inter-model 90 % range than CMIP5. The former spans from -63 % to -4 % and the latter from -56 % to -11 %. For the low emission scenario CMIP6 mean JJA precipitation declines by -7 % (90 % between -23 % and +17 %) and CMIP5 by -4 % (90 % within -19 % to +16 %). In winter and by the end of the century, CMIP6 precipitation declines by -8 % (90 % between -20 % and +5 %) and CMIP5 by -9 % (90 % between -31 % to +4 %) under the high emission scenario. For the low emission scenario in DJF, CMIP6 shows a mean +2 % precipitation increase (90 % between -11 % and +18 %) and CMIP5 a -1 % decline (90 % within -15 % to 9 %). The rest of seasons and scenarios show mean PR declines beginning from the mid-term period onwards. Nevertheless, during the 21st century under the low emission scenario a slight increase in mean winter precipitation is projected. HighResMIP near-term

https://doi.org/10.5194/esd-2021-65
Preprint. Discussion started: 30 July 2021

Earth System Dynamics
Discussions

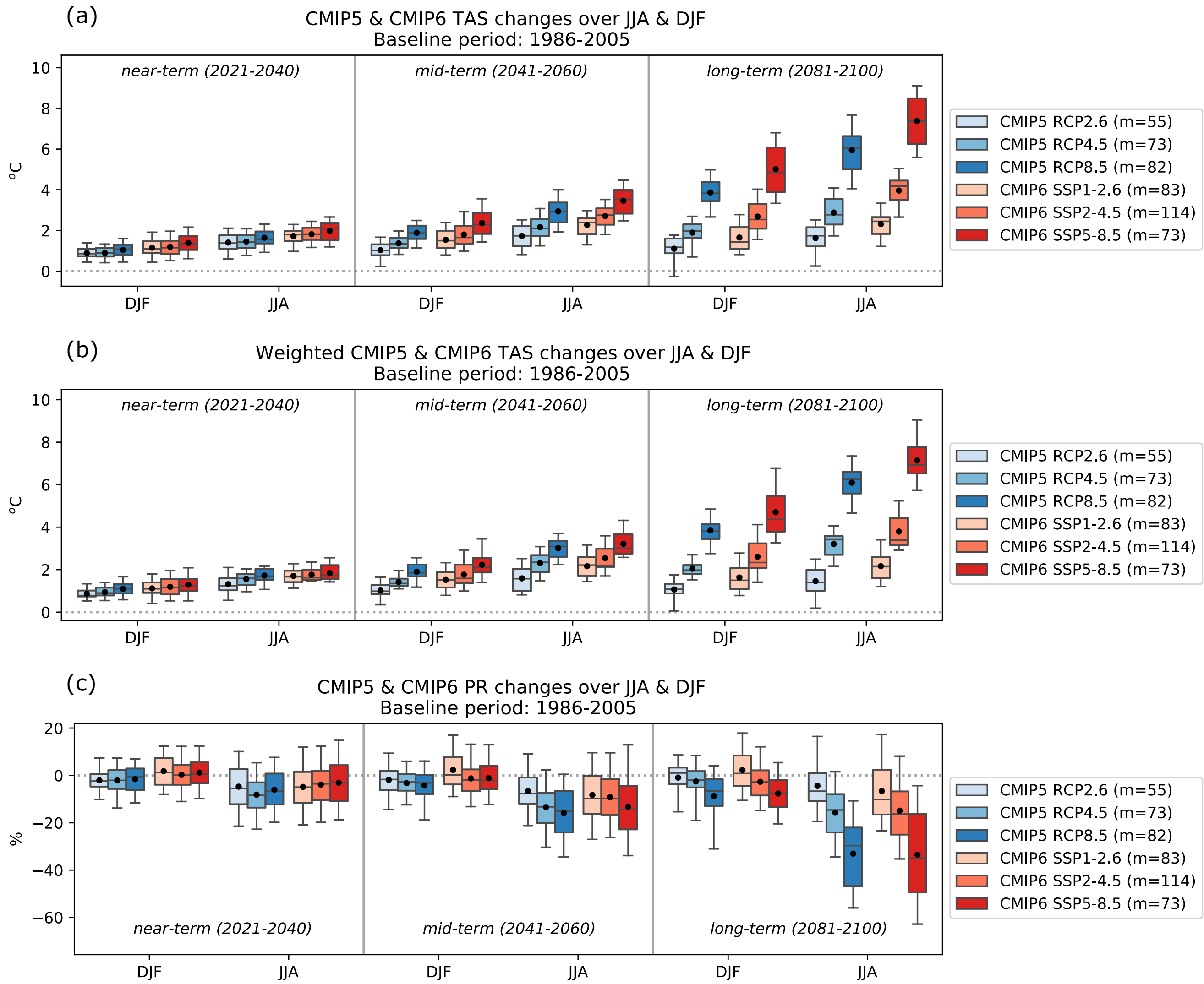

Figure 3. CMIP5 and CMIP6 summer and winter projected changes for the near, mid and long-term periods with respect to the baseline period considering the 2.6, 4.5 and 8.5 Wm^-2 RCP and SSP radiative forcing scenarios for (a) unweighted TAS (b) weighted TAS and (c) unweighted PR. The black horizontal line in the boxes represents the median and the black dot is the mean. The interquartile range (IQR) and whiskers are defined by the 25th-75th and 5th-95th percentiles, respectively. The number of members in the boxplot distributions is represented by *m* in the legend.

projections of PR change are contained within the CMIP6 ensemble (Fig. S3(b,d)). Generally, the signal is weak and the inter-model spread is wide for all multi-model ensembles, therefore we will later present the statistical robustness and significance of changes.

https://doi.org/10.5194/esd-2021-65
Preprint. Discussion started: 30 July 2021

Earth System Dynamics Discussions

The inter-model spread grows larger with emissions both for TAS and PR (Fig. 3(a,c)). To check the influence of the equilibrium climate sensitivity (ECS) on the increasing inter-model spread, the same plot is computed with a subset of CMIP5 and CMIP6 models with ECSs constrained between 2.6 and 3.3 (rather than the original 2.1 to 4.7 ECS range from CMIP5 (Meehl et al., 2020) and the 1.8 to 5.6 ECS range from CMIP6 (Hausfather, 2019)). Figure S6 shows that ensembles which contain models with similar ECS see a reduction in inter-model spread growth alongst time for the higher emission scenarios.

Figures 4 and 5 show the spatial distribution of the changes projected by the high emission scenario for JJA TAS and PR.

Summer warming is significant and robust for the three future periods in the Mediterranean region (see Fig. 4). HighResMIP warming shows many non-statistically significant grid points, due to the ensemble only having 4 models as it reduces the degrees of freedom for the t-Student test and makes it harder to reject the hypothesis that the ensemble means for the baseline and the future periods are the same. As seen before, CMIP6 warms more than CMIP5 and at a faster rate. Nevertheless, there is good spatial agreement between the warming projected by the CMIP experiments over the Mediterranean region. The Iberian peninsula, the Balkans and Eastern Europe are the regions with the largest mean summer warming, with values reaching over 8 ºC.

The remaining scenarios also project robust and significant warming for summer throughout the century with a tendency of smaller positive trends by 2050 (not shown). CMIP6 keeps projecting higher warming than CMIP5 again with a similar spatial warming pattern. The regions with larger warming are the Iberian peninsula and the Balkans.

The temperature changes during winter for the high emission scenario are shown in Fig. S8. The north-eastern Mediterranean shows the largest projected warming in winter (4.5 ºC according to CMIP5 and 6 ºC to CMIP6). For the near-term, HighResMIP shows a slightly larger TAS increase than CMIP6 in eastern Europe. The rest of scenarios agree with the spatial distribution of changes but with lower warming magnitudes (not shown).

In contrast to temperature, precipitation changes only get more robust and significant with time (see Fig. 5). Changes projected for the long-term during summer and under the 8.5 Wm^{-2} scenarios indicate significant and robust precipitation declines for most of the region. Note that neither significant nor robust changes are projected in the south and east Mediterranean mainly due to the already low or non-existent precipitation during summer, according to the climatology observed by CRU. Both CMIPs agree on the south-western Iberian peninsula having the strongest precipitation decline, with long-term CMIP6 changes ranging from -50 to -60 % and CMIP5 by -30 to -40 % for the high emission scenario. Despite lower forcing scenarios projecting non-significant changes (except the western Mediterranean for long-term SSP2-4.5) and less inter-model agreement, they agree on a general precipitation decline (not shown). The HighResMIP projections concord with CMIP6 mean magnitudes and spatial pattern for most of the seasons in the near-term period (the large amount of non-robust and non-significant grid points must be noted).

Precipitation changes in winter are different from those in summer (see Fig. S9). The southern part of the domain is expected to see a significant and robust precipitation decline in the long-term of up to -20 to -40% over northern Africa. The north of the Mediterranean is located in a transition zone, as precipitation in areas over the Pyrenees, Alps and Balkans is projected to increase and in areas under 38º N is projected to decrease, causing changes for the Iberian, Italian and Balkan peninsulas

https://doi.org/10.5194/esd-2021-65
Preprint. Discussion started: 30 July 2021

Earth System Dynamics
Discussions
Open Access

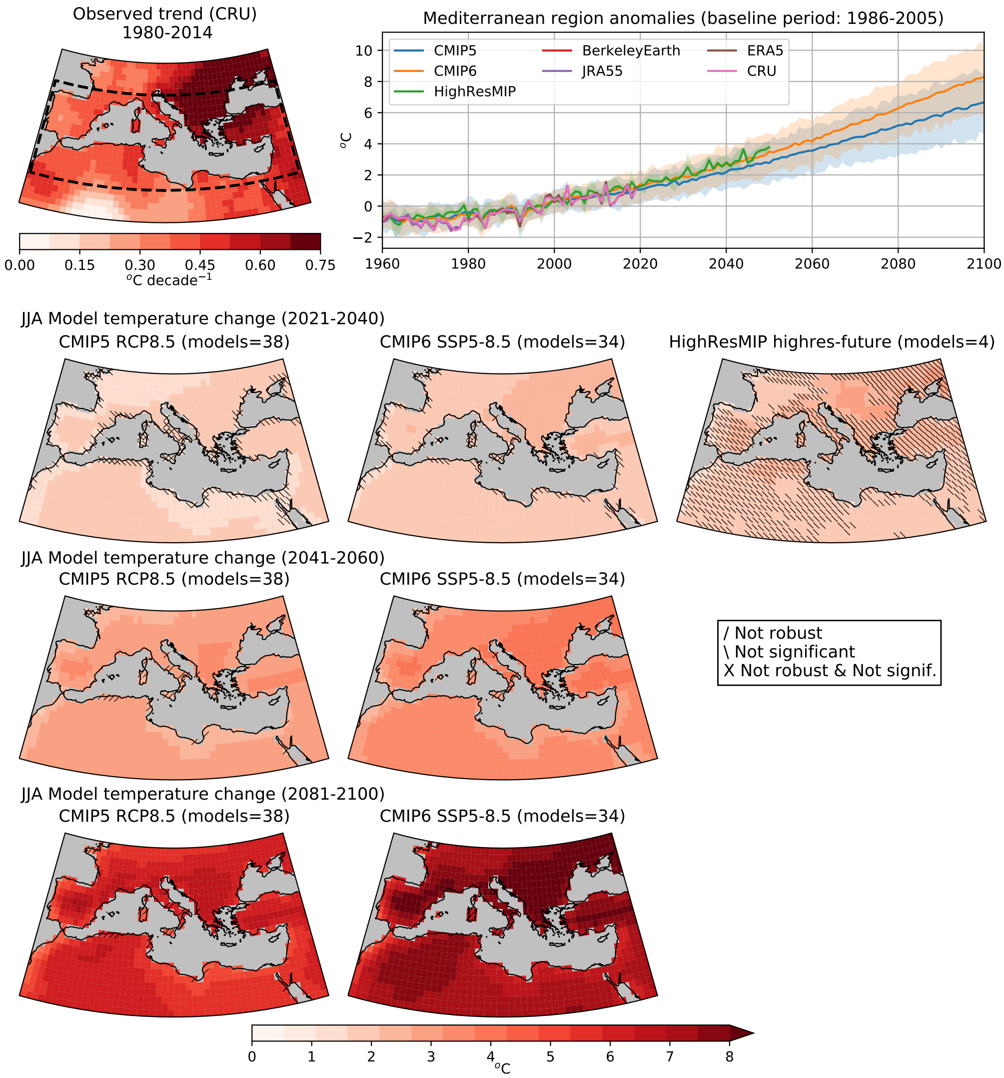

Figure 4. Summer TAS change according to CMIP5, CMIP6 and HighResMIP ensemble means (columns) for the three relevant future periods (rows), under the RCP8.5 and SSP5-8.5 scenarios. The time series plot shows the anomalies in the Mediterranean region with respect to the period 1986-2005 for the multi-model ensembles and the observational references. A solid line indicates the one-member-per-model ensemble mean and the shaded region indicates the 5th-95th percentiles range. CRU trend for the period 1980-2014 is shown along with the dashed line which bounds the Mediterranean region. Non-significant coastline grid points are due to differences in the original grid resolutions between models. Coarse models have masked data in complex coastline regions once regridded, making the ensemble smaller and therefore reducing the degrees of freedom for the t-Student test.

to remain uncertain. In comparison to CMIP5, CMIP6 shows more significant and robust changes over the region and wider 5-95th percentile spreads. This remains true for the rest of the scenarios (not shown).

https://doi.org/10.5194/esd-2021-65
Preprint. Discussion started: 30 July 2021

Earth System Dynamics
Discussions
Open Access

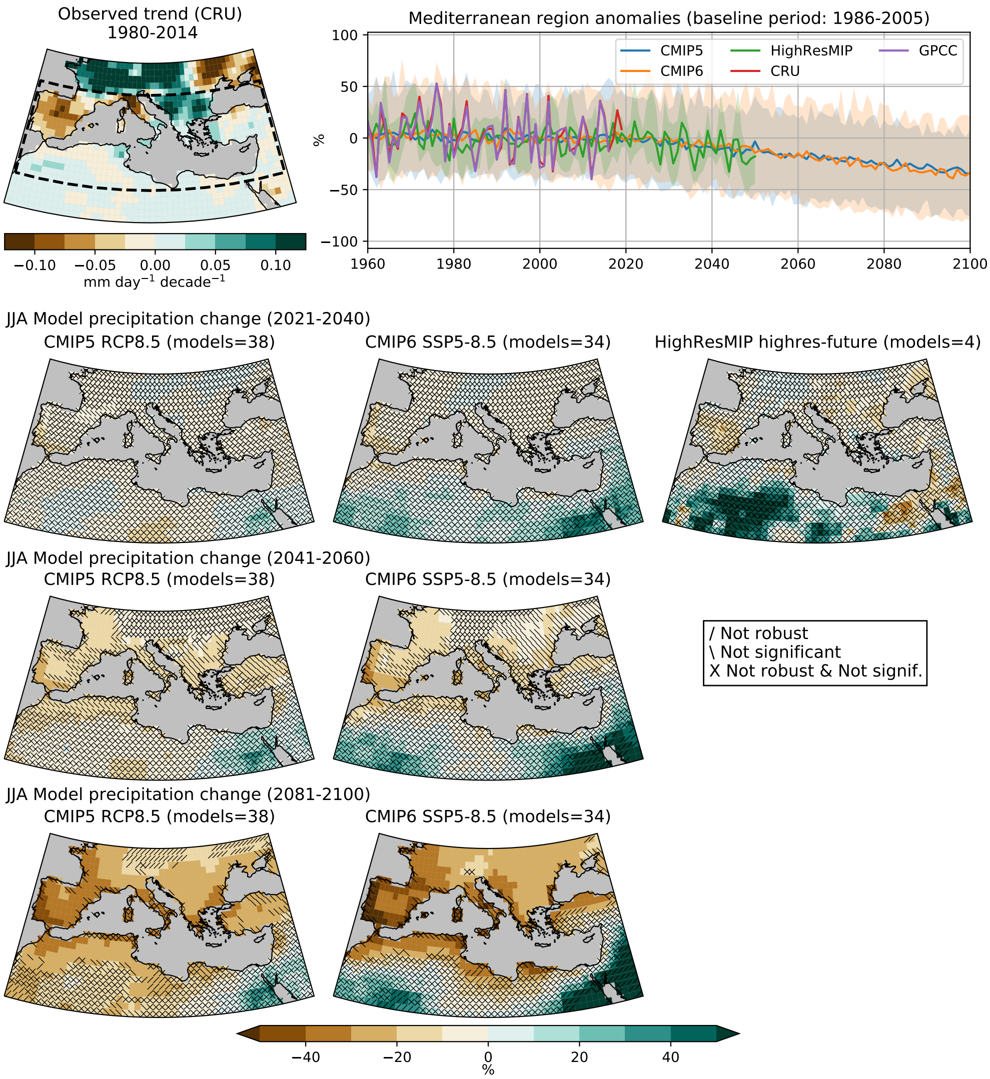

Figure 5. Same as Fig. 4 for summer precipitation and showing CRU in the top left panel.

The observed winter precipitation variability in the time series is stronger than the simulated 90 % range, this suggests that models fail to fully capture the amplitude of precipitation inter-annual oscillations during winter.

3.3 Weighting projections

The models of CMIP ensembles perform very differently depending on the computed diagnostic, and some models share similarities. Section 1 of the supplementary material explains in further detail how differently models represent the observed climate over the Mediterranean region, justifying the need to constraint the projection ensembles.

https://doi.org/10.5194/esd-2021-65
Preprint. Discussion started: 30 July 2021

We obtain new projections from applying the performance and independence weighting method to the CMIP5 and CMIP6 ensembles. Figure 3.b shows the distribution of temperature changes in the weighted ensembles for the three emission scenarios and the three future periods. The weighting increases the CMIP5 mean and median projections while at the same time decreasing the CMIP6 mean and median projections, bringing the two ensemble means closer together. Generally, the high emission scenario means are the ones that see larger reductions in CMIP6 ensemble, e.g. differences between the unweighted and weighted ensemble means of around -0.3, -0.2 and -0.1 ºC in summer and winter for SSPs 5-8.5, 2-4.5 and 1-2.6, respectively. The IQRs are generally narrowed for all seasons, and scenarios except for the mid and late century summer SSP2-4.5, SSP1-2.6 and RCP2.6 scenarios. The 90 % spreads are slightly reduced or maintained, exceptions are the CMIP6 DJF long-term distributions and the CMIP6 JJA low and mid emission scenarios for the mid-term. The 75-95th percentile range in the weighted CMIP6 ensemble increases while the 5-25th percentile range decreases, generating a skewed CMIP6 weighted distribution towards smaller warming. Weighting the CMIP5 ensemble leads to a more constrained distribution.

The weighted temperature projections in winter show similar responses as in summer: CMIP6 mean signal decreases while CMIP5 increases, making the differences between both mean distributions smaller. In some cases the weighting did not lead to significant alterations of the projected inter-model spread, suggesting that uncertainties in the temperature changes are well sampled by the original ensembles. In contrast, the large IQR of CMIP6 model projections in the long-term is reduced by half, and the CMIP5 90 % inter-model spread narrows up to 1 ºC, after weighting. Nevertheless, even if the probability of a future extreme-warming decreases, such temperature increases are still considered valid by the weighted ensemble. Generally speaking, the 90 % inter-model spreads are maintained while the IQRs narrow.

4 Discussion

Projections obtained from climate multi-model ensembles contain various sources of uncertainties. Different modelling methods and emission scenarios (e.g land use, GHG emissions...) lead to different results (Tebaldi and Knutti, 2007). We use different multi-model ensembles and radiative forcing scenarios to consider as many factors as possible contributing to the uncertainty of the Mediterranen climate change projections. Additionally, a weighting method constraining the projections has been applied to reduce uncertainty in the projections.

Compared to the global warming signal, we have shown that the Mediterranean mean temperature changes are stronger in summer and almost identical in winter, irrespective of the considered scenario, timeframe and multi-model ensemble. This hotspot is projected to enhance over the 21st century under the scenarios RCP8.5, SSP5-8.5, RCP4.5 and SSP2-4.5, and to diminish from the mid to long term under the RCP2.6 or SSP1-2.6 scenarios. Interestingly, the multi-model ensemble means of the low emission scenario project a recovery of the precipitation decline towards the end of the century, suggesting that precipitation could be restored to historical values relatively fast in the Mediterranean region if strict mitigation policies are applied. Previous studies also have identified the Mediterranean warming amplification (Lionello and Scarascia, 2018; Zittis et al., 2019), but it must be stressed that this enhanced warming does not apply to the winter season. Even if CMIP6 projections are warmer, the Mediterranean-Global warming ratio is not enhanced with respect to CMIP5, meaning that the

https://doi.org/10.5194/esd-2021-65
Preprint. Discussion started: 30 July 2021

Earth System Dynamics
Discussions

warming relationship between the Mediterranean and the rest of the globe is maintained for both multi-model ensembles. The precipitation projections in the region show a drying trend compared to meridional changes (30º N-45º N latitudinal belt), enhancing the climate change hotspot.

Temperature projections show that the warming over the 21st century is larger when stronger radiative forcing scenarios are applied, consistent with basic radiative forcing theory (Wallace and Hobbs, 2006). There is confidence in a precipitation decline for the high emission scenario over all the Mediterranean region in summer and only in the south during winter. Conclusions should be drawn carefully from precipitation as there is a large inter-model spread. For other seasons and scenarios, precipitation declines are projected, although results are uncertain due to large spread and low significance and robustness over most of the region. Regarding HighResMIP, the HR near-term precipitation and temperature changes generally fall within the CMIP6 ensemble distribution and no clear improvement could be seen from the increased resolution, probably due to the small number of HighResMIP models available for the assessment, and the focus on larger scale changes and temporal resolutions.

As Tebaldi and Knutti (2007) suggest, historical temperature trends are a good indicator of projected future changes. A larger past temperature trend goes hand in hand with projections showing a higher warming (as seen in Fig. S3(a,c)). This is true for all scenarios and seasons, confirming that the historical temperature trend is a good indicator of the magnitude of future warming.

The largest source of uncertainty to determine the warming and precipitation change by the mid and long-term periods is the emission scenario. To illustrate the scenario uncertainty, let's take the range between the 5th and 95th percentile of the low (high) and high (low) emission scenario distributions for temperature (precipitation) changes. CMIP6 shows a range from 1ºC to 9ºC warming and -62% to 19% precipitation long-term changes in summer. CMIP5 ranges from 0.1ºC to 7.5ºC warming and -54% to 18%. This broad spectrum of possible futures has various possible outcomes associated. The inter-model spread grows at faster rates along the 21st century with higher radiative forcing, in part due to the different climate sensitivities of the models inside the ensemble, i.e. the differences between a low and a high climate sensitivity model will get amplified with larger radiative forcing.

The implications of an 8.5 Wm^{-2} increase in radiative forcing from preindustrial times by the end of the century could pose severe strains on: human health, due to heat-related illness (Lugo-Amador et al., 2004) and altered transmission of infectious diseases (Patz et al., 2005); food security due to crop pests and diseases (Newton et al., 2011) and productivity decline in many countries which economies depend on agriculture (Devereux and Edwards, 2004); and water insecurity due to droughts (Devereux and Edwards, 2004) and changing rainfall patterns in vulnerable regions (Sadoff and Muller, 2009). Note that the three climate change induced impacts defined above are closely intertwined and may increase existing scarcities.

In face of the very pessimistic future projected by the high emission scenario, some studies argue that 8.5 Wm^{-2} forcing is highly unlikely as it is based on an expansion of the coal use along the 21st century instead of on a reduction (Ritchie and Dowlatabadi, 2017a). In the context of energy transition and lowering demand of coal, the high emission scenario is often criticised (Ritchie and Dowlatabadi, 2017b). Nevertheless, studies on the carbon cycle discuss that CO_2 feedbacks might be underestimated in the GHG-concentration scenarios (Booth et al., 2017), and thus we've considered keeping the 8.5 scenarios as an extreme but yet possible future.

https://doi.org/10.5194/esd-2021-65
Preprint. Discussion started: 30 July 2021

Earth System Dynamics Discussions

The CMIP6 ensemble is known to have models with notably higher climate sensitivity than CMIP5, i.e. radiative forcing generates stronger changes and at a faster rate (Hausfather, 2019). Higher sensitivity can be due to model design or the definition of the radiative forcing scenario. Even if SSP and RCP scenarios are labelled after the radiative forcing (in Wm^{-2}) by the end of the century, the transient GHG concentrations are different (Meinshausen et al., 2011; Riahi et al., 2016). Wyser et al. (2020) suggests that running the same model with equal 2100 GHG concentrations from SSP and RCP (2.6, 4.5 and 8.5 Wm^{-2}), leads to larger temperature changes when forcing the model with the former. Another aspect that might affect climate sensitivity is that CMIP6 models have improved the formulation of clouds and aerosols (Hausfather, 2019). Even if there is higher sensitivity to radiative forcing in some CMIP6 models, this behaviour is not reproduced by all of them, resulting in a larger inter-model spread compared to CMIP5. Assessing the weighted temperature ensemble, we found that the CMIP6 distribution shifts to lower changes, meaning that models showing larger TAS changes have been down-weighted, reducing the differences between CMIP6 and CMIP5 experiment medians and means. Studies have shown that some CMIP6 models with higher warming signals are poorly representing the historical climate (Tokarska et al., 2020). Nevertheless, CMIP6 still exhibits a large inter-model spread after weighting its members, signaling that those high-sensitivity model projections can still be reached (with lower probabilities). By using the inter-model spread as a sample of uncertainty, the weighted distribution from CMIP6 tells us that previous CMIP efforts might have been under-estimating the uncertainty of the projected warming.

Precipitation weighted projections are not shown in this study as we have no proof that the diagnostics used to assess temperature are relevant to evaluate the models precipitation response.

5 Conclusions

This study aims to analyse the projected temperature and precipitation changes by the CMIP5 and CMIP6 multi-model ensembles in the Mediterranean region. Different scenarios and seasons have been assessed to tackle the uncertainties inherent to ensemble projections. To complement the traditional information provided, a weighting method that accounts for historical performance and inter-independence of the models has been applied to offer an alternative view of the projections that is considered more trustworthy.

The Mediterranean is a climate-change hotspot due to the amplified warming and drying when compared to the large-scale climate behaviour. The amplified warming of the Mediterranean especially affects temperature during summer and not in winter. Comparing the Mediterranean hotspot in CMIP5 and CMIP6 we found that the ratio of warming amplification is similar for both multi-model means, meaning that no enhanced warming is projected by the CMIP6 ensemble, but it is rather the consequence of a globally warmer ensemble.

Conclusions must be drawn carefully from multi-model ensembles as the single models perform very differently and might share dependencies with each other. Model agreement gives high confidence in significant and robust warming affecting the entire Mediterranean region along the 21st century caused by anthropogenic emissions. The Balkans during winter and the Balkan and Iberian peninsulas during summer are expected to be the most affected regions. Precipitation changes are less robust and significant and show greater spatial heterogeneity than the warming. Significant and robust declines in precipitation

https://doi.org/10.5194/esd-2021-65
Preprint. Discussion started: 30 July 2021

are expected to affect the Mediterranean in summer and the southern part in winter by the end of the 21st century if high emission scenarios are considered. The warming combined with a precipitation decline could put under strain the whole region, especially the south, which has less resources to adapt to the changing climate. The biggest source of uncertainty to determine the magnitude of TAS and PR changes is the emission scenario, which will depend on the future policies and measures for mitigation followed. Part of the increasing inter-model spread with time is related to the wide range of ECS values among the ensemble members.

A weighting method has been applied to reduce the uncertainty caused by models that poorly represent key aspects of the historical climate or by the high dependence of the results provided by families of models (that might be overrepresented in the multi-model ensemble). Based on the constrained projections we conclude that CMIP6 overestimates warming in the Mediterranean and its 25th to 50th percentile inter-model spread. CMIP5 slightly underestimates warming and generally overestimates the IQR inter-model spread. The weighted projections are relevant because they help to reconcile the conclusions extracted from the last two CMIP phases, reducing future uncertainties of climate change. The fact that CMIP6's 90 % spread range is unaltered, shows that the climate uncertainty might have been underestimated in previous, less physically advanced, CMIP exercises, which displayed smaller inter-model spread when constrained.

Further work is required for the weighting method to identify the most relevant diagnostics that best assess historical precipitation model performance. As spatial heterogeneities can be seen in the Mediterranean region, we suggest to consider subregions for the Mediterranean to extract more user-relevant information from the constrained projections. Both RCM and longer high-resolution global model simulations will have to be considered to better understand the influence of some important local features in the Mediterranean region like complex orography and coastlines.

Code and data availability. The tool used for the diagnostics (ESMValTool) can be found at https://github.com/ESMValGroup/. ESMValTool v2.2 is publicly available on Zenodo at https://zenodo.org/record/4562215#.YOWlhTqxVH4 (Andela et al., 2021). The source code of the ESMValCore package, which is installed as a dependency of the ESMValTool v2.3, is also publicly available on Zenodo at https://zenodo.org/record/4947127#.YOa2BsBR1QI (Andela et al., 2021b). ESMValTool and ESMValCore are developed on the GitHub repositories available at https://github.com/ESMValGroup. The observational data used: GPCC (doi:10.5676/DWD_GPCC/FD_M_V2020_025), CRU (https://crudata.uea.ac.uk/cru/data/hrg/cru_ts_4.04/cruts.2004151855.v4.04/, https://doi.org/10.1038/s41597-020-0453-3.), JRA55 (https://jra.kishou.go.jp/JRA-55/index_en.html#reanalysis), ERA5 (https://doi.org/10.1002/qj.3803), BerkeleyEarth (http://berkeleyearth.lbl.gov/auto/Global/Gridded/Complete_TAVG_LatLong1.nc), HadSLP (https://doi.org/10.1175/JCLI3937.1). CMIP data: all the CMIP5 and 6 datasets were downloaded from the Earth System Grid Federation (ESGF). The models used are listed in Appendix A. For CMIP6, the DOIs of the datasets from the ESGF can be obtained in Identifier DOI after clicking on "show citation" from the following url https://esg-dn1.nsc.liu.se/search/cmip6-liu/?source_id=ACCESS-CM2,ACCESS-ESM1-5,AWI-CM-1-1-MR,BCC-CSM2-MR,CAMS-CSM1-0,CAS-ESM2-0,CESM2-WACCM,CIESM,CMCC-CM2-SR5,CNRM-CM6-1,CNRM-ESM2-1,CanESM5-CanOE,EC-Earth3,FGOALS-f3-L,FGOALS-g3,FIO-ESM-2-0,GFDL-ESM4,GISS-E2-1-G,HadGEM3-GC31-LL,INM-CM4-8,INM-CM5-0,IPSL-CM6A-LR,KACE-1-0-G,KIOST-ESM,MCM-UA-1-0,MIROC-ES2H,MPI-ESM1-2-HR,MPI-ESM1-2-LR,MRI-ESM2-0,NorESM2-LM,NorESM2-MMUKESM1-0-LL&experiment_id=historical,ssp126,ssp245,ssp585&variant_label=r1i1p1f1,r1i1p1f2,r1i1p1

https://doi.org/10.5194/esd-2021-65
Preprint. Discussion started: 30 July 2021

f3,r2i1p1f1,r2i1p1f2,r2i1p1f3,r3i1p1f1,r3i1p1f2,r4i1p1f1,r4i1p1f2,r5i1p1f1,r5i1p1f2,r6i1p1f1,r6i1p1f2,r7i1p1f1,r7i1p1f2,r8i1p1f1,r8i1p1f2,r9i1p1f1,r9i1p1f2&table_id=Amon&variable_id=tas

The ESMValTool recipes and the code for the diagnostics can be found at http://doi.org/10.23728/b2share.ec53147170d6440aa3da66fdb8879398

Additional figures not shown in the main text or the supplementary material can be found in the figure repository built with a shiny app following the link https://earth.bsc.es/shiny/medprojections-shiny_app/.

Appendix A: Model data summary

A summary of all the initial-condition runs from the multi-model ensembles CMIP5, CMIP6 and HighResMIP, for the three radiative scenarios used in this study can be found in Table A1.

Appendix B: Diagnostics, σ_d and σ_s of the weighting method

This Appendix aims to describe the methodology behind the performance and independence weighting. First, we will explain the diagnostics chosen to compute the distances and secondly how to obtain the two constant shape parameters from equation (1).

As the aim is to obtain weighted projections from a multi-model ensemble, the diagnostics to assess performance and independence must be relevant for the used variable. The weighting is going to be optimised for temperature projections and therefore variables TAS and PSL from the historical period (1980-2014) will be used, as these variables are relevant for the projected temperature ((Merrifield et al., 2020), (Brunner et al., 2020)). In order for CMIP5 to comply with the historical reference period, the diagnostics will include the first years of the scenario experiments (2006-2014). As there is a unique ensemble of members for each project, scenario and season, each ensemble will have its own set of weights.

The diagnostics used are differences, climatologies, trends, and variability. According to Tebaldi and Knutti (2007), TAS historical trends have an evident physical link and high correlation with future projected warming. The trend is defined by the linear ordinary least square regression fit for each grid point with time as independent variable during the reference period (TREND); the climatologies are computed as the time mean of each grid point over the reference period (CLIM); the differences are computed by subtracting the area averaged climatology to each grid point's reference period climatology (DIFF) and the variability is obtained with the mean inter-annual standard deviation for each grid point (STD). As the trend is not relevant for PSL, it is not computed (Merrifield et al., 2020).

When assessing performance, the aim is to identify the models that more faithfully represent the historical climate. As all our results are computed as differences from the historical period, model biases in the climatology shouldn't be relevant. That is why the diagnostics used for performance weighting are TAS-TREND, TAS-DIFF, TAS-STD, PSL-DIFF and PSL-DIFF. Differently, the aim of weighting for independence is to identify members that have similar traits. Biases in models should be similar for dependent models (Merrifield et al., 2020), therefore we use CLIM for temperature and sea level pressure (TAS-CLIM and PSL-CLIM) to compute the distances S_{ij} from equation (1). Computing the climatology over relatively long periods

https://doi.org/10.5194/esd-2021-65
Preprint. Discussion started: 30 July 2021

Earth System Dynamics
Discussions

Table A1. Summary of the members used in this study from CMIP5, CMIP6 and HighResMIP. The columns display the emssion scenarios.

CMIP5	RCP2.6	RCP4.5	RCP8.5	CMIP6	SSP1-2.6	SSP2-4.5	SSP5-8.5
ACCESS1-0	-	r1i1p1	r1i1p1	ACCESS-CM2	r1i1p1f1	r(1-2)i1p1f1	r1i1p1f1
ACCESS1-3	-	r1i1p1	r1i1p1	ACCESS-ESM1-5	r(1-3)i1p1f1	r(1-10)i1p1f1	r(1-3)i1p1f1
BCC-CSM1-1	r1i1p1	r1i1p1	r1i1p1	AWI-CM-1-1-MR	r1i1p1f1	r1i1p1f1	r1i1p1f1
BCC-CSM1-1-M	r1i1p1	r1i1p1	r1i1p1	BCC-CSM2-MR	r1i1p1f1	r1i1p1f1	r1i1p1f1
BNU-ESM	r1i1p1	r1i1p1	r1i1p1	CanESM5	r(1-10)i1p1f1	r(1-10)i1p1f1	r(1-10)i1p1f1
CanESM2	r(1-5)i1p1	r(1-5)i1p1	r(1-5)i1p1	CanESM5-CanOE	r(1-3)i1p1f1	r(1-3)i1p1f1	r(1-3)i1p1f1
CCSM4	r(1-5)i1p1	r(1-5)i1p1	r(1-5)i1p1	CAS-ESM2-0	-	r(1,3)i1p1f1	-
CESM1-BGC	-	r1i1p1	r1i1p1	CESM2	r1i1p1f1	r(1,4,10-11)i1p1f1	r(1,2)i1p1f1
CESM1-CAM5	r(1-3)i1p1	r(1-3)i1p1	r(1-3)i1p1	CESM2-WACCM	r1i1p1f1	r(1-3)i1p1f1	r1i1p1f1
CMCC-CESM	-	-	r1i1p1	CIESM	-	r1i1p1f1	r1i1p1f1
CMCC-CM	-	r1i1p1	r1i1p1	CMCC-CM2-SR5	r1i1p1f1	r1i1p1f1	r1i1p1f1
CMCC-CMS	-	r1i1p1	r1i1p1	CNRM-CM6-1	r(1-6)i1p1f2	r(1-6)i1p1f2	r1i1p1f2
CNRM-CM5	r1i1p1	-	r(1-2,4,6,10)i1p1	CNRM-CM6-1-HR	r1i1p1f2	r1i1p1f2	r1i1p1f2
CSIRO-Mk3-6-0	r(1-10)i1p1	r(1-10)i1p1	r(1-10)i1p1	CNRM-ESM2-1	r(1-5)i1p1f2	r(1-5)i1p1f2	r1i1p1f2
EC-Earth	r(8,12)i1p1	r(2,6-9,12-14)i1p1	r(1,2,6,8,9,12,13)i1p1	EC-Earth3	r(4,6,9,11,13,15)i1p1f1	r(2,7,18-24)i1p1f2	r(4,6,9,11,13,15)i1p1f1
FGOALS-s2	-	r1i1p1	r(1-3)i1p1	FGOALS-g3	r1i1p1f1	r(1-4)i1p1f1	r1i1p1f1
FIO-ESM	r(1:3)i1p1	r(1-3)i1p1	r(1-3)i1p1	FGOALS-f3-L	r1i1p1f1	r1i1p1f1	r1i1p1f1
GFDL-CM3	-	r1i1p1	r1i1p1	FIO-ESM-2-0	r(1-3)i1p1f1	r(1-3)i1p1f1	r(1-3)i1p1f1
GFDL-ESM2G	r1i1p1	-	r1i1p1	GFDL-ESM4	r1i1p1f1	r1i1p1f1	r1i1p1f1
GFDL-ESM2M	r1i1p1	-	r1i1p1	GISS-E2-1-G	r1i1p3f1	-	r1i1p3f1
GISS-E2-H	r1i1p1	r(1-3,5)i1p1	r(1-2)i1p1	HadGEM3-GC31-LL	r1i1p1f3	r1i1p1f3	r(1-3)i1p1f3
GISS-E2-H-CC	-	-	r1i1p1	INM-CM4-8	r1i1p1f1	r1i1p1f1	r1i1p1f1
GISS-E2-R	r1i1p1	r(2,6)1i1p3	r(1-2)i1p1	INM-CM5-0	r1i1p1f1	r1i1p1f1	r1i1p1f1
GISS-E2-R-CC	-	-	r1i1p1	IPSL-CM6A-LR	r(1-4,6)i1p1f1	r(1-6,10,11,14,22,25)i1p1f1	r1i1p1f1
HadGEM2-AO	r1i1p1	-	r1i1p1	KACE-1-0-G	r(1-2)i1p1f1	r(1,3)i1p1f1	r1i1p1f1
HadGEM2-ES	r(1-4)i1p1	r(1-4)i1p1	r(1-4)i1p1	KIOST-ESM	-	r1i1p1f1	-
INMCM4	-	r1i1p1	r1i1p1	MCM-UA-1-0	r1i1p1f1	r1i1p1f1	r1i1p1f1
IPSL-CM5A-LR	r(1-4)i1p1	r3i1p1	r(1-4)i1p1	MIROC6	r(1-3)i1p1f1	r(1-3)i1p1f1	r(1-3)i1p1f1
IPSL-CM5A-MR	r1i1p1	r1i1p1	r1i1p1	MIROC-ES2L	r1i1p1f2	r1i1p1f2	r1i1p1f2
IPSL-CM5B-LR	-	r1i1p1	r1i1p1	MPI-ESM1-2-HR	r1i1p1f1	r1i1p1f1	r1i1p1f1
MIROC-ESM	r1i1p1	r1i1p1	r1i1p1	MPI-ESM1-2-LR	r(1-10)i1p1f1	r(1-10)i1p1f1	r(1-10)i1p1f1
MIROC-ESM-CHEM	r1i1p1	r1i1p1	r1i1p1	MRI-ESM2-0	r1i1p1f1	r1i1p1f1	r1i1p1f1
MIROC5	r(2-3)1i1p1	r(2-3)i1p1	r(2-3)i1p1	NESM3	r(1-2)i1p1f1	r(1-2)i1p1f1	r(1-2)i1p1f1
MPI-ESM-LR	r(1-3)i1p1	r(1-3)i1p1	r(1-3)i1p1	NorESM2-LM	r1i1p1f1	r(1-3)i1p1f1	r1i1p1f1
MPI-ESM-MR	r1i1p1	r(1-3)i1p1	r1i1p1	NorESM2-MM	r1i1p1f1	r1i1p1f1	r1i1p1f1
MRI-CGCM3	r1i1p1	r1i1p1	r1i1p1	UKESM1-0-LL	r(1-4,8)i1p1f2	r(1-4,8)i1p1f2	r(1-4,8)i1p1f2
MRI-ESM1	-	-	r1i1p1				
NorESM1-M	r1i1p1	r1i1p1	r1i1p1				
HighResMIP	**SSP5-8.5**		**SSP5-8.5**		**SSP5-8.5**		**SSP5-8.5**
CMCC-CM2-HR4	r1i1p1f1	CNRM-CM6-1	r1i1p1f1	EC-Earth3P	r3i1p2f1	HadGEMGE3-GC31-HM	r1i1p1f1
CMCC-CM2-VHR4	r1i1p1f1	CNRM-CM6-1-HR	r1i1p1f1	EC-Earth3P-HR	r2i1p2f1	HadGEMGE3-GC31-MM	r1i1p1f1

is a good approach as the internal variability gets minimised and ideally, it is the main attribute distinguishing two members of the same model (Hawkins and Sutton, 2011).

Finally, to compute the actual values of D_i and S_{ij} the single diagnostic distances (e.g. TAS-TREND, TAS-DIFF, PSL-DIFF...) must be combined. It is done by normalizing the single diagnostics with the median over all members and then averaging them.

https://doi.org/10.5194/esd-2021-65
Preprint. Discussion started: 30 July 2021

Earth System Dynamics Discussions

The shape parameters are constant thresholds that inform how large or small distances should be to determine performance (D_i) and independence (S_{ij}). If σ_d is overconstrained (small value), it will generate a very strict performance weighting as only members with very low values of D_i will receive any weight. Contrarily, if high values of σ_d are used, models with large distances will receive performance weight, leading to too permissive constraints. The independence shape parameter doesn't work in such a straightforward way, small values of σ_s could weight all models as being independent, as the distance to consider two members dependent would have to be too small. This could result in models receiving similar weights. A similar thing could happen but for the opposite reason if a large σ_s was used i.e. most models would seem dependent as large distances between members would be considered small enough. We therefore must find an optimal σ_s that is neither too small nor too large (Knutti et al., 2017).

The ensemble gives the necessary information to make a best guess of both shape parameters. Regarding the performance parameter, Knutti et al. (2017) suggests applying perfect model tests for a range of σ_d candidates to obtain the optimal magnitude. The candidates are values between the 10% and 200% of the median D_i distance. Consecutively, all members in the ensemble are once taken as the reference while the rest are weighted following equation (1) with D_i being the distance between the perfect member and the member i. The σ_d candidates are iteratively tested for all perfect model tests until the smallest σ_d that makes 80% of the perfect models fall in between the 10th and 90th percentiles of their respective weighted ensembles is found. The diagnostics used in the test are the same as the ones used to weight performance but computed for the future periods (2041-2060 and 2081-2100) as we want σ_d to be based on the uncertainties of the future projection ensemble. The average σ_d between both periods is used for its corresponding season, scenario and CMIP ensemble.

The parameter σ_s is informed by models with more than one initial-condition run. Ideally, members from the same model should be considered completely dependent as their modelling assumptions are the same, even though internal variability makes the runs differ. The independence weighting should identify when initial-condition runs from the same model are added or subtracted from an ensemble. If the independence weights (equation (1) denominator) are calculated for an ensemble with one member per model (w_j^{ind}) and then all the available members of a model j are added to the ensemble (E_j represents the amount of members added), the average independence weights of model j ($\tilde{w}_j^{ind}$) are expected to decrease by a ratio $1 : E_j$. Additionally, including members of a model j to the ensemble should have a minimal effect on the independence weights of the rest of models i represented by only one member in the ensemble.

The optimal σ_s is found via an iterative process for a range of σ_s candidates, looking for the one that minimizes the sum $\epsilon_1 + \epsilon_2$, where ϵ_1 and ϵ_2 are defined as (Brunner et al., 2019):

$$mean_j \left[w_j^{ind}(\sigma_s) + E_j - \tilde{w}_j^{ind}(\sigma_s) \right]^2 = \epsilon_1$$
$$mean_j \left\{ mean_i \left[w_{i \neq j}^{ind}(\sigma_s) - \tilde{w}_{i \neq j}^{ind}(\sigma_s) \right]^2 \right\} = \epsilon_2 \ \forall \text{j}$$

https://doi.org/10.5194/esd-2021-65
Preprint. Discussion started: 30 July 2021

Earth System Dynamics
Discussions

Author contributions. JC, FD and MJ designed the study. JC developped and ran the diagnostics, and wrote the initial manuscrip. MJ helped in the Figures production. MJ, FD, RM and JC contributed to the interpretation of the results and improvement of the manuscript. PB and MS contributed to the download and fixes of the datasets used in this study.

Competing interests. The authors declare that they have no conflict of interest.

Acknowledgements. We acknowledge the World Climate Research Programme, which, through its Working Group on Coupled Modelling, coordinated and promoted CMIP5 and CMIP6. We thank the climate modeling groups for producing and making available their model output, the Earth System Grid Federation (ESGF) for archiving the data and providing access, and the multiple funding agencies who support CMIP5 and CMIP6 and ESGF. We also thank the European Center for Medium-Range Weather Forecast (ECMWF), the Japan Meteorological Agency (JMA), the University of East Anglia (UEA), the Deutscher Wetterdienst (DWD), Berkeley Earth and the Met Office (UKMO) for providing ERA5, JRA55, CRU, GPCC, BerkeleyEarth and HadSLP2 reanalysis/observational data, respectively. We acknowledge the Earth System Evaluation Tool (ESMValTool) community for the development and distribution of the tool, and we sincerely thank the technical support from Saskia Loosveldt-Tomas and Javier Vegas-Regidor (BSC-CNS) with the tool. The work in this paper was partly supported by the European Commission H2020 project EUCP (grant no. 776613).

https://doi.org/10.5194/esd-2021-65
Preprint. Discussion started: 30 July 2021

References

Allan, R. and Ansell, T.: A new globally complete monthly historical gridded mean sea level pressure dataset (HadSLP2): 1850-2004, J. Climate, 19, 5816–5842, https://doi.org/10.1175/JCLI3937.1, 2006.

Barros, V., Field, C., Dokken, D., Mastrandrea, M., Mach, K., Bilir, T., Chatterjee, M., Ebi, K., Estrada, Y., Genova, R., Girma, B., Kissel, E., Levy, A., MacCracken, S., Mastrandrea, P., and L.L.White: IPCC, 2014: Impacts, Adaptation, and Vulnerability. Part B: Regional Aspects. Contribution of Working Group II to the Fifth Assessment Report of the Intergovernmental Panel on Climate Change, Tech. rep., 2014.

Boé, J. and Terray, L.: Land-sea contrast, soil-atmosphere and cloud-temperature interactions: Interplays and roles in future summer European climate change, Clim. Dynam., 42, 683–699, https://doi.org/10.1007/s00382-013-1868-8, 2014.

Booth, B. B. B., Harris, G. R., Murphy, J. M., House, J. I., Jones, C. D., Sexton, D., and Sitch, S.: Narrowing the Range of Future Climate Projections Using Historical Observations of Atmospheric CO 2 , J. Climate, 30, 3039–3053, https://doi.org/10.1175/jcli-d-16-0178.1, 2017.

Brogli, R., Kröner, N., Sørland, S. L., Lüthi, D., and Schär, C.: The role of hadley circulation and lapse-rate changes for the future European summer climate, J. Climate, 32, 385–404, https://doi.org/10.1175/JCLI-D-18-0431.1, 2019.

Brunner, L., Lorenz, R., Zumwald, M., and Knutti, R.: Quantifying uncertainty in European climate projections using combined performance-independence weighting, Environ. Res. Lett., 14, https://doi.org/10.1088/1748-9326/ab492f, 2019.

Brunner, L., Pendergrass, A., Lehner, F., Merrifield, A., Lorenz, R., and Knutti, R.: Reduced global warming from CMIP6 projections when weighting models by performance and independence, Earth Syst. Dynam., 6, 1–23, https://doi.org/10.5194/esd-2020-23, 2020.

Collins, M., Knutti, R., Dufresne, J.-L., Fichefet, T., Friedlingstein, P., Gao, X., and Al., E.: Long-term climate change: Projections, commitments and irreversibility, Climate change 2013: The physical science basis. Contribution of Working Group I to the Fifth Assessment Report of the Intergovernmental Panel on Climate Change, Tech. rep., 2013.

Cox, P. M., Huntingford, C., and Williamson, M. S.: Emergent constraint on equilibrium climate sensitivity from global temperature variability, Nature, 553, 319–322, https://doi.org/10.1038/nature25450, 2018.

Cramer, W., Guiot, J., Fader, M., Garrabou, J., Gattuso, J. P., Iglesias, A., Lange, M. A., Lionello, P., Llasat, M. C., Paz, S., Peñuelas, J., Snoussi, M., Toreti, A., Tsimplis, M. N., and Xoplaki, E.: Climate change and interconnected risks to sustainable development in the Mediterranean, Nat. Clim. Change, 8, 972–980, https://doi.org/10.1038/s41558-018-0299-2, 2018.

Dennis, S.: The Climate Data Guide: Regridding Overview, https://climatedataguide.ucar.edu/climate-data-tools-and-analysis/regridding-overview., 2014.

Deser, C., Lehner, F., Rodgers, K. B., Ault, T., Delworth, T. L., DiNezio, P. N., Fiore, A., Frankignoul, C., Fyfe, J. C., Horton, D. E., Kay, J. E., Knutti, R., Lovenduski, N. S., Marotzke, J., McKinnon, K. A., Minobe, S., Randerson, J., Screen, J. A., Simpson, I. R., and Ting, M.: Insights from Earth system model initial-condition large ensembles and future prospects, Nat. Clim. Change, 10, 277–286, https://doi.org/10.1038/s41558-020-0731-2, 2020.

Devereux, S. and Edwards, J.: Climate Change and Food Security, IDS Bull.-I Dev. Stud., pp. 22–30, https://doi.org/https://doi.org/10.1111/j.1759-5436.2004.tb00130.x, 2004.

Eyring, V., Bony, S., Meehl, G. A., Senior, C. A., Stevens, B., Stouffer, R. J., and Taylor, K. E.: Overview of the Coupled Model Intercomparison Project Phase 6 (CMIP6) experimental design and organization, Geosci. Model Dev., 9, 1937–1958, https://doi.org/10.5194/gmd-9-1937-2016, 2016.

https://doi.org/10.5194/esd-2021-65
Preprint. Discussion started: 30 July 2021

Garfinkel, C. I., Adam, O., Morin, E., Enzel, Y., Elbaum, E., Bartov, M., Rostkier-Edelstein, D., and Dayan, U.: The role of zonally averaged climate change in contributing to intermodel spread in CMIP5 predicted local precipitation changes, J. Climate, 33, 1141–1154, https://doi.org/10.1175/JCLI-D-19-0232.1, 2020.

Gleick, P. H.: Water, drought, climate change, and conflict in Syria, Weather, Climate, and Society, 6, 331–340, https://doi.org/10.1175/WCAS-D-13-00059.1, 2014.

Haarsma, R. J., Roberts, M. J., Vidale, P. L., Catherine, A., Bellucci, A., Bao, Q., Chang, P., Corti, S., Fučkar, N. S., Guemas, V., Von Hardenberg, J., Hazeleger, W., Kodama, C., Koenigk, T., Leung, L. R., Lu, J., Luo, J. J., Mao, J., Mizielinski, M. S., Mizuta, R., Nobre, P., Satoh, M., Scoccimarro, E., Semmler, T., Small, J., and Von Storch, J. S.: High Resolution Model Intercomparison Project (HighResMIP v1.0) for CMIP6, Geosci. Model Dev., 9, 4185–4208, https://doi.org/10.5194/gmd-9-4185-2016, 2016.

Hall, A., Cox, P., Huntingford, C., and Klein, S.: Progressing emergent constraints on future climate change, Nat. Clim. Change, 9, 269–278, https://doi.org/10.1038/s41558-019-0436-6, 2019.

Harris, I., Osborn, T. J., Jones, P., and Lister, D.: Version 4 of the CRU TS monthly high-resolution gridded multivariate climate dataset, Q. J. Roy. Meteor. Soc., 7, 1–18, https://doi.org/10.1038/s41597-020-0453-3, 2020.

Hausfather, Z.: CMIP6: the next generation of climate models explained, https://www.carbonbrief.org/cmip6-the-next-generation-of-climate-models-explained, 2019.

Hawkins, E. and Sutton, R.: The potential to narrow uncertainty in projections of regional precipitation change, Clim. Dynam., 37, 407–418, https://doi.org/10.1007/s00382-010-0810-6, 2011.

Herger, N., Abramowitz, G., Sherwood, S., Knutti, R., Angélil, O., and Sisson, S. A.: Ensemble optimisation, multiple constraints and overconfidence: a case study with future Australian precipitation change, Clim. Dynam., 53, 1581–1596, https://doi.org/10.1007/s00382-019-04690-8, 2019.

Hersbach, H., Bell, B., Berrisford, P., Hirahara, S., Horányi, A., Muñoz-Sabater, J., Nicolas, J., Peubey, C., Radu, R., Schepers, D., Simmons, A., Soci, C., Abdalla, S., Abellan, X., Balsamo, G., Bechtold, P., Biavati, G., Bidlot, J., Bonavita, M., De Chiara, G., Dahlgren, P., Dee, D., Diamantakis, M., Dragani, R., Flemming, J., Forbes, R., Fuentes, M., Geer, A., Haimberger, L., Healy, S., Hogan, R. J., Hólm, E., Janisková, M., Keeley, S., Laloyaux, P., Lopez, P., Lupu, C., Radnoti, G., de Rosnay, P., Rozum, I., Vamborg, F., Villaume, S., and Thépaut, J. N.: The ERA5 global reanalysis, Earth Syst. Sci. Data, 146, 1999–2049, https://doi.org/10.1002/qj.3803, 2020.

Iturbide, M., Gutiérrez, J. M., Alves, L. M., Bedia, J., Cimadevilla, E., Cofiño, A., Cerezo-Mota, R., Di Luca, A., Faria, S. H., Gorodetskaya, I., Hauser, M., Herrera, S., Hewitt, H., Hennessy, K., Jones, R., Krakovska, S., Manzanas, R., Marínez-Castro, D., Narisma, G. T., Nurhati, I., Pinto, I., Seneviratne, S., van den Hurk, B., and Vera, C.: An update of IPCC climate reference regions for subcontinental analysis of climate model data: Definition and aggregated datasets, Earth Syst. Sci. Data, pp. 1–16, https://doi.org/10.5194/essd-2019-258, 2020.

Knutti, R., Sedláček, J., Sanderson, B. M., Lorenz, R., Fischer, E. M., and Eyring, V.: A climate model projection weighting scheme accounting for performance and interdependence, Geophys. Res. Lett., 44, 1909–1918, https://doi.org/10.1002/2016GL072012, 2017.

Kobayashi, S., Ota, Y., Harada, Y., Ebita, A., Moriya, M., Onoda, H., Onogi, K., Kamahori, H., Kobayashi, C., Endo, H., Miyaoka, K., and Kiyotoshi, T.: The JRA-55 reanalysis: General specifications and basic characteristics, Int. J. Climatol., 93, 5–48, https://doi.org/10.2151/jmsj.2015-001, 2015.

Langenbrunner, B. and Neelin, J. D.: Pareto-Optimal Estimates of California Precipitation Change, Geophys. Res. Lett., 44, 12,436–12,446, https://doi.org/10.1002/2017GL075226, 2017.

Lehner, F., Deser, C., Maher, N., Marotzke, J., Fischer, E., Brunner, L., Knutti, R., and Hawkins, E.: Partitioning climate projection uncertainty with multiple Large Ensembles and CMIP5/6, Earth Syst. Dynam., pp. 1–28, https://doi.org/10.5194/esd-2019-93, 2020.

Lionello, P. and Scarascia, L.: The relation between climate change in the Mediterranean region and global warming, Reg. Environ. Change, 18, 1481–1493, https://doi.org/10.1007/s10113-018-1290-1, 2018.

Longobardi, A. and Villani, P.: Trend analysis of annual and seasonal rainfall time series in the Mediterranean area, Int. J. Climatol., 30, 1538–1546, https://doi.org/10.1002/joc.2001, 2010.

Lorenz, R., Herger, N., Sedláček, J., Eyring, V., Fischer, E. M., and Knutti, R.: Prospects and Caveats of Weighting Climate Models for Summer Maximum Temperature Projections Over North America, Journal of Geophysical Research: Atmospheres, 123, 4509–4526, https://doi.org/10.1029/2017JD027992, 2018.

Lugo-Amador, N. M., Rothenhaus, T., and Moyer, P.: Heat-related illness, Emerg. Med. Clin. N. Am., 22, 315–327, https://doi.org/10.1016/j.emc.2004.01.004, 2004.

McSweeney, C. F., Jones, R. G., Lee, R. W., and Rowell, D. P.: Selecting CMIP5 GCMs for downscaling over multiple regions, Clim. Dynam., 44, 3237–3260, https://doi.org/10.1007/s00382-014-2418-8, 2015.

Meehl, G. A., Senior, C. A., Eyring, V., Flato, G., Lamarque, J. F., Stouffer, R. J., Taylor, K. E., and Schlund, M.: Context for interpreting equilibrium climate sensitivity and transient climate response from the CMIP6 Earth system models, Science Advances, 6, 1–11, https://doi.org/10.1126/sciadv.aba1981, 2020.

Meinshausen, M., Smith, S. J., Calvin, K., Daniel, J. S., Kainuma, M. L., Lamarque, J., Matsumoto, K., Montzka, S. A., Raper, S. C., Riahi, K., Thomson, A., Velders, G. J., and van Vuuren, D. P.: The RCP greenhouse gas concentrations and their extensions from 1765 to 2300, Climatic Change, 109, 213–241, https://doi.org/10.1007/s10584-011-0156-z, 2011.

Merrifield, A. L., Brunner, L., Lorenz, R., Medhaug, I., and Knutti, R.: An investigation of weighting schemes suitable for incorporating large ensembles into multi-model ensembles, Earth SystGlobal Planet. Change. Dynam., pp. 807–834, 2020.

Newton, A. C., Johnson, S. N., and Gregory, P. J.: Implications of climate change for diseases, crop yields and food security, Euphytica, 179, 3–18, https://doi.org/10.1007/s10681-011-0359-4, 2011.

O'Neill, B. C., Tebaldi, C., Van Vuuren, D. P., Eyring, V., Friedlingstein, P., Hurtt, G., Knutti, R., Kriegler, E., Lamarque, J. F., Lowe, J., Meehl, G. A., Moss, R., Riahi, K., and Sanderson, B. M.: The Scenario Model Intercomparison Project (ScenarioMIP) for CMIP6, Geosci. Model Dev., 9, 3461–3482, https://doi.org/10.5194/gmd-9-3461-2016, 2016.

Paeth, H., Vogt, G., Paxian, A., Hertig, E., Seubert, S., and Jacobeit, J.: Quantifying the evidence of climate change in the light of uncertainty exemplified by the Mediterranean hot spot region, Energ. Econ., 151, 144–151, https://doi.org/10.1016/j.gloplacha.2016.03.003, 2017.

Patz, J. A., Campbell-Lendrum, D., Holloway, T., and Foley, J. A.: Impact of regional climate change on human health, Nature, 438, 310–317, https://doi.org/10.1038/nature04188, 2005.

Peña-Angulo, D., Vicente-Serrano, S. M., Domínguez-Castro, F., Murphy, C., Reig, F., Tramblay, Y., Trigo, R. M., Luna, M. Y., Turco, M., Noguera, I., Aznárez-Balta, M., García-Herrera, R., Tomas-Burguera, M., and El Kenawy, A.: Long-term precipitation in Southwestern Europe reveals no clear trend attributable to anthropogenic forcing, Environ. Res. Lett., 15, https://doi.org/10.1088/1748-9326/ab9c4f, 2020.

Riahi, K., van Vuuren, D. P., Kriegler, E., Edmonds, J., O'Neill, B. C., Fujimori, S., Bauer, N., Calvin, K., Dellink, R., Fricko, O., Lutz, W., Popp, A., Cuaresma, J. C., KC, S., Leimbach, M., Jiang, L., Kram, T., Rao, S., Emmerling, J., Ebi, K., Hasegawa, T., Havlik, P., Humpenöder, F., Da Silva, L. A., Smith, S., Stehfest, E., Bosetti, V., Eom, J., Gernaat, D., Masui, T., Rogelj, J., Strefler, J., Drouet, L., Krey, V., Luderer, G., Harmsen, M., Takahashi, K., Baumstark, L., Doelman, J. C., Kainuma, M., Klimont, Z., Marangoni, G., Lotze-Campen, H., Obersteiner, M., Tabeau, A., and Tavoni, M.: The Shared Socioeconomic Pathways and their energy, land use, and greenhouse

https://doi.org/10.5194/esd-2021-65
Preprint. Discussion started: 30 July 2021

gas emissions implications: An overview, Global Environmental Change, 42, 153–168, https://doi.org/10.1016/j.gloenvcha.2016.05.009, 2016.

Righi, M., Andela, B., Eyring, V., Lauer, A., Predoi, V., Schlund, M., Vegas-Regidor, J., Bock, L., Brötz, B., de Mora, L., Diblen, F., Dreyer, L., Drost, N., Earnshaw, P., Hassler, B., Koldunov, N., Little, B., Loosveldt Tomas, S., and Zimmermann, K.: Earth System Model Evaluation Tool (ESMValTool) v2.0 - technical overview, Geosci. Model Dev., 13, 1179–1199, https://doi.org/10.5194/gmd-13-1179-2020, 2020.

Ritchie, J. and Dowlatabadi, H.: The 1000 GtC coal question: Are cases of vastly expanded future coal combustion still plausible?, Energ. Econ., 65, 16–31, https://doi.org/10.1016/j.eneco.2017.04.015, 2017a.

Ritchie, J. and Dowlatabadi, H.: Why do climate change scenarios return to coal?, Energy, 140, 1276–1291, https://doi.org/10.1016/j.energy.2017.08.083, 2017b.

Rohde, R., Muller, R. A., Jacobsen, R., Muller, E., Perlmuller, S., Rosenfeld, A., Wurtele, J., Groom, D., and Wickham, C.: A New Estimate of the Average Earth Surface Land Temperature Spanning 1753 to 2011, Geoinfor. Geostat. Overv., 1, 1–7, 2013.

Sadoff, C. and Muller, M.: Water management, water security and climate change adaptation: early impacts and essential responses., Global Water Partnership, 2009.

Schamm, K., Ziese, M., Becker, A., Finger, P., Meyer-Christoffer, A., Schneider, U., Schröder, M., and Stender, P.: Global gridded precipitation over land: A description of the new GPCC First Guess Daily product, Geophys. Res. Lett., 6, 49–60, https://doi.org/10.5194/essd-6-49-2014, 2014.

Taylor, K. E., Stouffer, R. J., and Meehl, G. A.: An overview of CMIP5 and the experiment design, B. Am. Meteorol. Soc., 93, 485–498, https://doi.org/10.1175/BAMS-D-11-00094.1, 2012.

Tebaldi, C. and Knutti, R.: The use of the multi-model ensemble in probabilistic climate projections, Ocean Model., 365, 2053–2075, https://doi.org/10.1098/rsta.2007.2076, 2007.

Tokarska, K. B., Stolpe, M. B., Sippel, S., Fischer, E. M., Smith, C. J., Lehner, F., and Knutti, R.: Past warming trend constrains future warming in CMIP6 models, Science Advances, 6, 1–14, https://doi.org/10.1126/sciadv.aaz9549, 2020.

Tsujino, H., Urakawa, S., Nakano, H., Small, R. J., Kim, W. M., Yeager, S. G., Danabasoglu, G., Suzuki, T., Bamber, J. L., Bentsen, M., Böning, C. W., Bozec, A., Chassignet, E. P., Curchitser, E., Boeira Dias, F., Durack, P. J., Griffies, S. M., Harada, Y., Ilicak, M., Josey, S. A., Kobayashi, C., Kobayashi, S., Komuro, Y., Large, W. G., Le Sommer, J., Marsland, S. J., Masina, S., Scheinert, M., Tomita, H., Valdivieso, M., and Yamazaki, D.: JRA-55 based surface dataset for driving ocean–sea-ice models (JRA55-do), J. Hydrometeorol., 130, 79–139, https://doi.org/10.1016/j.ocemod.2018.07.002, 2018.

Tuel, A. and Eltahir, E. A. B.: Why Is the Mediterranean a Climate Change Hot Spot?, J. Climate, 33, 5829–5843, https://doi.org/10.1175/jcli-d-19-0910.1, 2020.

van Vuuren, D. P., Edmonds, J., Kainuma, M., Riahi, K., Thomson, A., Hibbard, K., Hurtt, G. C., Kram, T., Krey, V., Lamarque, J. F., Masui, T., Meinshausen, M., Nakicenovic, N., Smith, S. J., and Rose, S. K.: The representative concentration pathways: An overview, Climatic Change, 109, 5–31, https://doi.org/10.1007/s10584-011-0148-z, 2011.

Voosen, P.: New climate models predict a warming surge, Science, https://doi.org/doi:10.1126/science.aax7217, 2019.

Wallace, J. M. and Hobbs, P. V.: Atmospheric science: An introductory survey, Amsterdam: Elsevier Academic Press, 2006.

Wang, C., Soden, B. J., Yang, W., and Vecchi, G. A.: Compensation Between Cloud Feedback and Aerosol-Cloud Interaction in CMIP6 Models, Geophys. Res. Lett., 48, 1–10, https://doi.org/10.1029/2020GL091024, 2021.

Weedon, G. P., Gomes, S., Viterbo, P., Shuttleworth, W. J., Blyth, E., Österle, H., Adam, J. C., Bellouin, N., Boucher, O., and Best, M.: Creation of the WATCH Forcing Data and Its Use to Assess Global and Regional Reference Crop Evaporation over Land during the Twentieth Century, J. Hydrometeorol., 12, https://doi.org/10.1175/2011JHM1369.1, 2011.

Wyser, K., Kjellström, E., Koenigk, T., Martins, H., and Döscher, R.: Warmer climate projections in EC-Earth3-Veg: The role of changes in the greenhouse gas concentrations from CMIP5 to CMIP6, Environ. Res. Lett., 15, https://doi.org/10.1088/1748-9326/ab81c2, 2020.

Zittis, G., Hadjinicolaou, P., Klangidou, M., Proestos, Y., and Lelieveld, J.: A multi-model, multi-scenario, and multi-domain analysis of regional climate projections for the Mediterranean, Reg. Environ. Change, 19, 2621–2635, https://doi.org/10.1007/s10113-019-01565-w, 2019.